# GEOELECTRIC SOUNDING AND HYDROCHEMICAL ANALYSIS FOR VULNERABILITY ASSESSMENT OF FUTA CAMPUS USING MODIFIED LE GRAND MODEL

.


## ABSTRACT

The work is aim at assessing possible impact of FUTA dumpsite on groundwater resources within the campus. Vertical electrical sounding was done across the study area in 94 locations. Three to five geoelectric layers were delineated in the study area. The layers correspond to the topsoil, weathered layer (sandy clay and clayey sand), lateritic weathered layer, partially weathered basement/partially fractured basement and the presumed fresh bedrock. The layer's resistivity varies respectively from 38 - 845 ohm-m, 9 - 7490 ohm-m, 41 - 90224 ohm-m, 60 - 15191 ohm, 162 - 99668 ohm-m, while the layer thickness ranges from 0.4 - 5.2 m, 0.9 - 24.1 m, 2.8 - 30.4 m and 4.3 - 41.6 m. The VES also results enabled the delineation of aquifer layer(s) where present, identification of the overlaying lithology above the aquifer layer across the area, determination of the transverse resistance, aquifer overburden longitudinal conductance, coefficient of anisotropy and VES distances from the dumpsite. These parameters were combined using the Le Grand model chart to evaluate and generate aquifer venerability model across the study area. The campus was classified into four zones of vulnerability; low, moderate, high, and very high. The current dumpsite is located in low vulnerability zones. The elevation map shows that the dump site is located at relatively low elevation to other areas, thus eliminating outward flow of leachate to other areas. The aquifer vulnerability model map (AVMM) was validated using physio-chemical analysis parameters (total dissolved solid, conductivity and total hardness) obtained from water samples from 8 different wells in the study area. The AVMM has 100% agreement with the water physio-chemical analysis. All water samples analysis results are within the WHO permissible limits.



*Keywords: Geoelectric, Hydrochemical, Vulnerability, Assessment and Le Grand Model*


## 1. INTRODUCTION

Economic development, urbanization and population growth always leads to increase in waste production, as nations and cities offer more products and services to their citizens and participate in global trade and exchange. However, the management of waste becomes a major problem for many cities, including those in Nigeria when the ratio of solid waste generation exceeds the capacity of city authorities to handle (1 - 4). In low-income countries like Nigeria, open dumping is the most common method of waste disposal, resulting in environmental crises and health hazards such as contamination of groundwater resources and air pollution arising from waste burning (5, 6).

It is important to choose locations of dumpsites or landfills carefully using scientific approach to avoid subjecting the available groundwater resources to risk of contamination (3 - 5).
Waste management involves the collection, transportation, processing, recycling and disposal of waste materials, all of which are aim at reducing impacts waste on human health and the environment (37,38). Poor solid waste management can lead to significant environmental and health hazards, such as contamination of groundwater by leachate and

.

degradation of raw materials (6). Groundwater is a crucial natural resources that many people depend on for their domestics, industrial and agricultural use (7, 8). However, the quality of groundwater resources is decreasing globally and Nigeria is not exempted due to anthropogenic activities and some natural processes (such as saltwater intrusion, flood, earth quake, volcanic eruption among others) resulting into water-borne diseases and deaths.

## 2. STUDY AREA

The study area is the campus of Federal University of Technology, Akure (FUTA) in Akure South Local Government area of Ondo State. It falls between 0735382 and 0735511 (31N, Northing) and 0807887 and 0808003 (Easting) based on the universal traverse mercator (Fig. 1). The area is moderately undulating with surface elevation ranging between 353 and 410 m above mean sea level (Fig. 2). The area is located within the sub-equatorial climate belt of the tropical rain forest vegetation. The area is characterized by wet and dry seasons. The geology of the FUTA campus is characterized by the presence of granitic plutons that crosscut the metamorphic rocks of the migmatite-gneiss-quartzite complex rocks (Fig. 3).

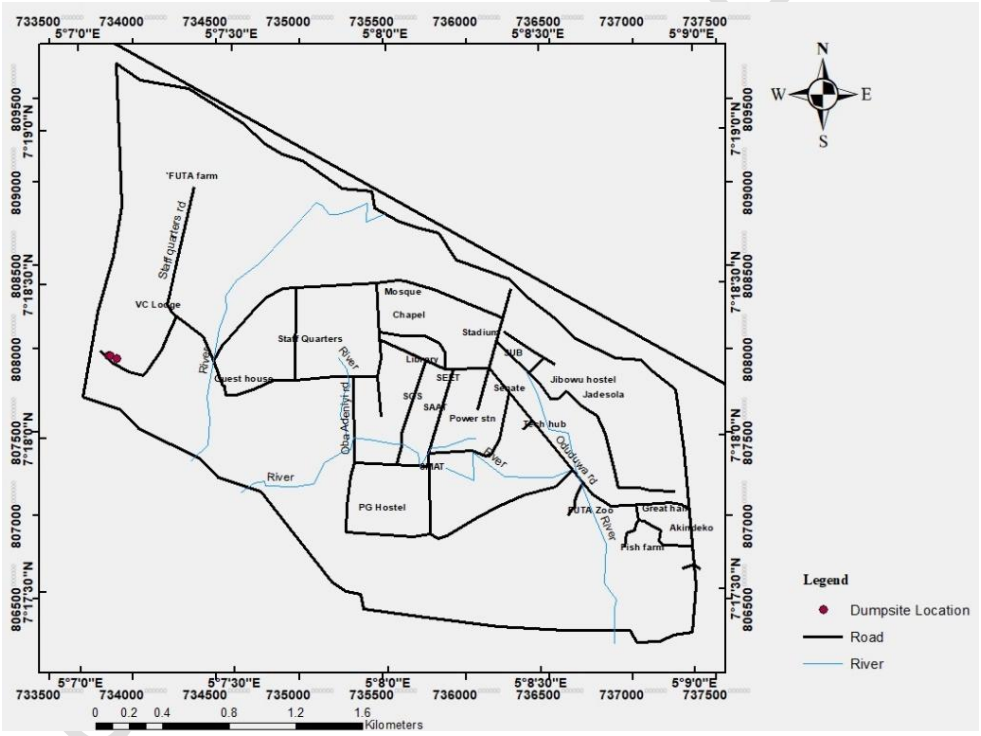


Fig. 1: Layout Map of Federal University of Technology, Akure (FUTA), Nigeria campus

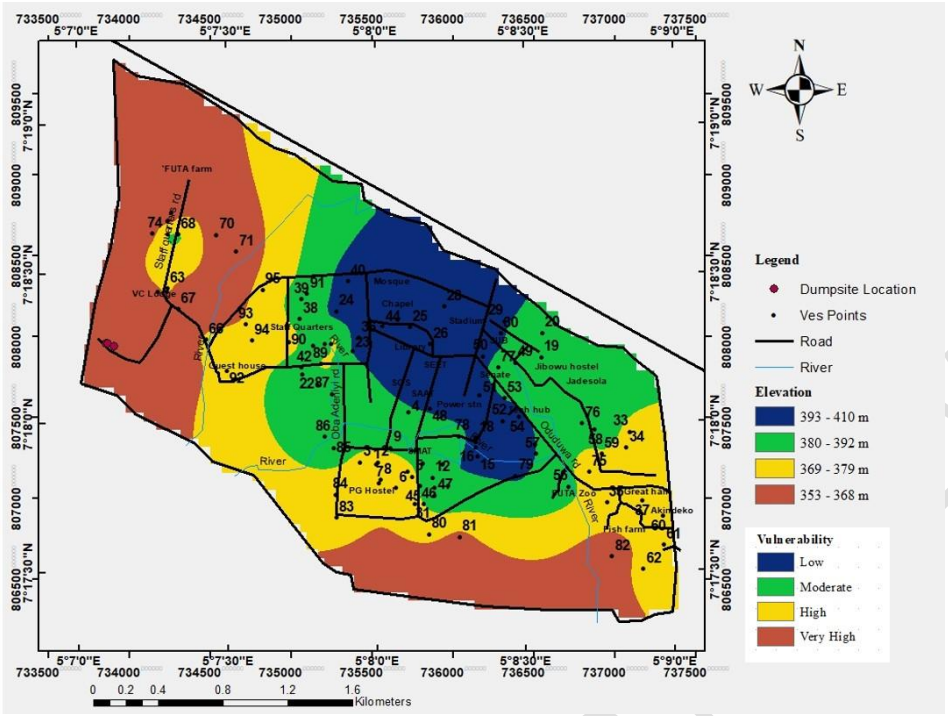


Fig. 2: Elevation Map of the Study Area

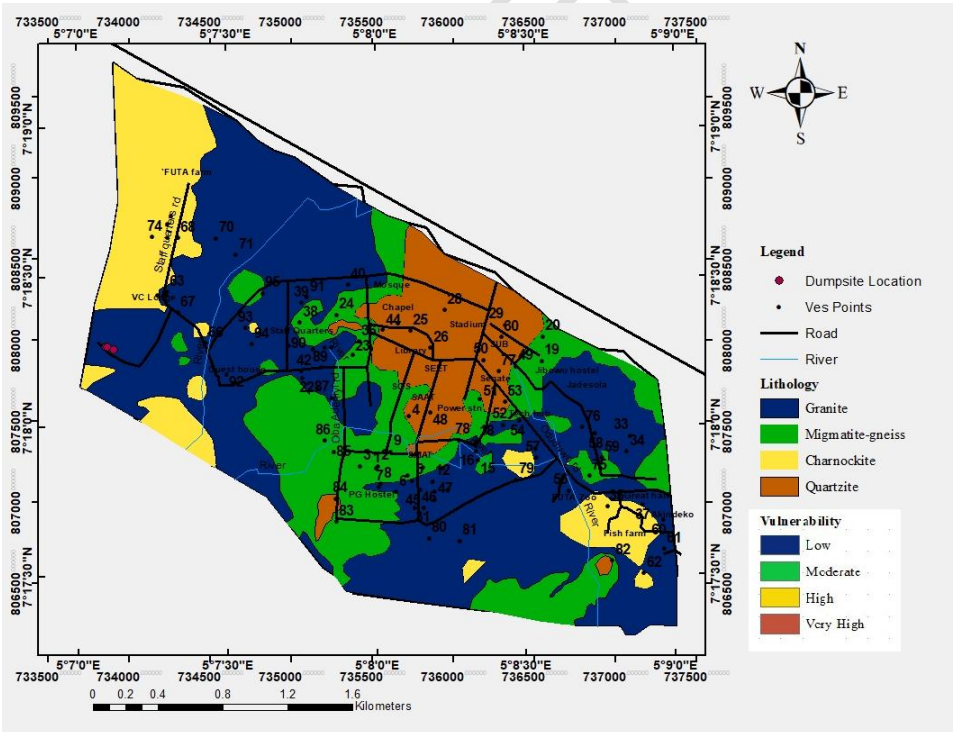


Fig. 3:Geological Map of the Study Area (9)

## 3. MATERIAL AND METHODS

FUTA campus is a fast growing community that generates waste, it is therefore essential to assess possible impact of the campus' dumpsite on the groundwater resources. The results of this work will assist the University Authority to deploy appropriate measures to mitigate against any possible contamination threat to the groundwater resources within the campus. The objectives utilized in achieving this aim involves; delineating different geoelectric layers beneath the study area, identifying the aquifer layer where present, delineating the overlaying lithology above the aquifer layer across the area, determining distance of the dumpsite from each VES locations across the area, determine second order geoelectric parameters (overburden longitudinal conductance, transverse resistance and coefficient of anisotropy values) across the area, modifying the Le Grand model to suit basement complex environment and geoelectric data in order to evaluate aquifer venerability across the area (10, 11) and validating the modified vulnerability model using physio-chemical analysis parameters.

Multi Criteria Decision Analysis (MCDA) methods have been used extensively for vulnerability prediction especially in basement complex terrains. Varieties of MCDA so far deployed includes but not limited to the following; AVI (Aquifer vulnerability index; 12), GOD (groundwater occurrence, overlying lithology and depth to the aquifer; 8, 13, 14), GODL (groundwater occurrence, overlying lithology, depth to the aquifer and lithology; 15), GODT (geology, overlying layer, depth to aquifer layer and topography; 16), AHP-GODT (17), GLSI (geoelectric layer susceptibility indexing; 8, 18), SINCTAS (19 - 26) and DRASTIC (depth to groundwater, net recharge, lithology of the aquifer, soil texture, topography, lithology of vadoze zone and hydraulic conductivity; 27 - 30).

MCDA application can be very tedious and prone to human error when parameters weight assignments are based on expert opinions. Consequently, Le Grand pollution correlation chart (Table 1 and Fig. 4) which does not require assigning weight to the parameters under consideration was adopted and adapted in this work (Le Grand, 1964; Salufu et. al., 2022). The Le Grand pollution correlation chart uses parameters that are directly related to factors that initiate soil, surface and groundwater pollution. The Le Grand Vulnerability Model (LGVM) is a tool that was developed to assess the vulnerability of aquifer layers of in sedimentary communities close to landfills or dump sites (10, 11). The model uses a series of parameters to produce a vulnerability score for each community in the region. Other possible applications of LGVM chart are to evaluate the vulnerability of communities to hazards associated with hydroelectric development, to assess the vulnerability of sedimentary basins that are prone to landslides due to the instability of the underlying sedimentary layers and to evaluate the vulnerability of communities located near rivers that are prone to erosion or flooding caused by sediment deposition or changes in water levels.

The LGVM chart was adapted in this study to a basement environment. The parameters considered in this study are transverse resistance, longitudinal conductance, coefficient of anisotropy, aquifer overlying lithology and distance of each VES locations from dumpsite.



**Table 1: Le Grand Interpretation Table for Total Point in Pollution Evaluation (10)**

| S/N | Total Points | Possibility of Pollution |
|---|---|---|
| 1 | 0 - 4 | Imminent |
| 2 | 4 - 8 | Probable or possible |
| 3 | 8 - 12 | Possible but not likely |

| | | |
|---|---|---|
| 4 | 12 - 25 | Very improbable |
| 5 | 25 - 35 | Impossible |

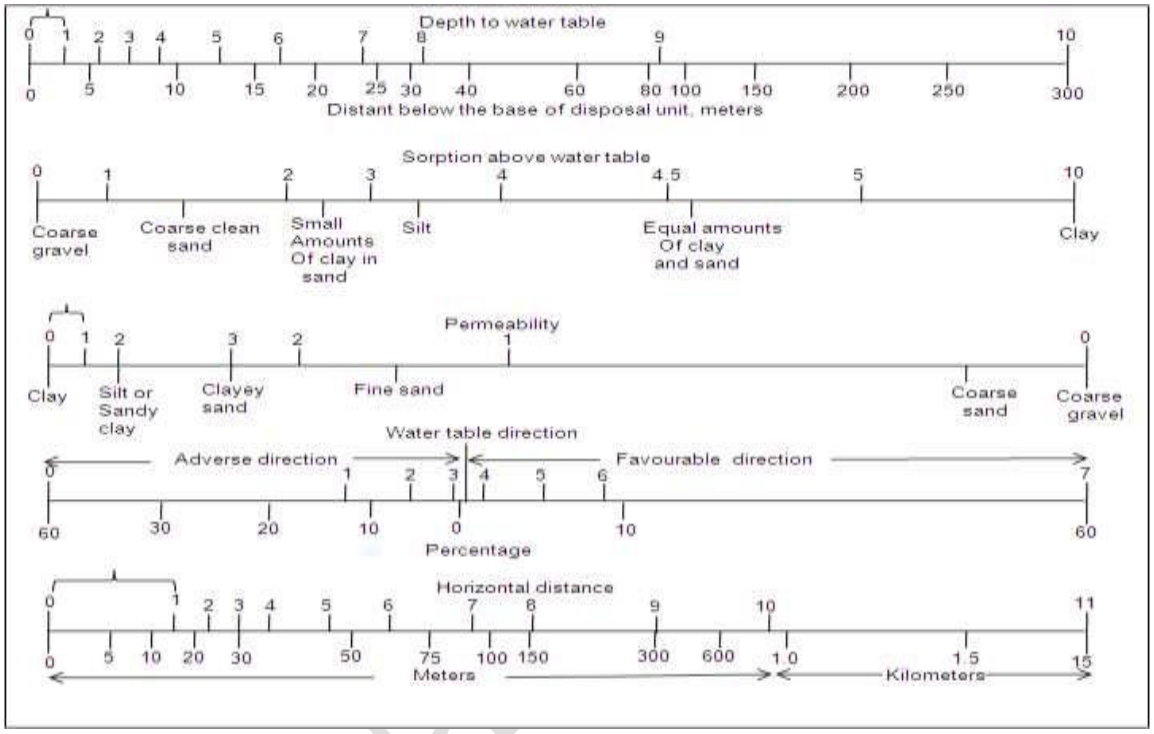


Fig. 4: Le Grand Pollution Chart**(10)**

The three (3) second order geoelectric parameters were also derived from the initial geoelectric parameters (Resistivity and Thickness values) using the following three (3) relationships;

**1. Longitudinal Conductance (S);**

$S = \sum \frac{h_i}{\rho_i} = \frac{h_1}{\rho_1} + \frac{h_2}{\rho_2} + \frac{h_3}{\rho_3} + \cdots \frac{h_n}{\rho_n}$ (31, 32) (1)

Where,

$h_i$ is layer thickness

$\rho_i$ is layer resistivity

**2. Transverse Resistance (T);**

$T = \sum h_i \rho_i = h_1\rho_1 + h_2\rho_2 + \cdots + h_n\rho_n$ (31, 32) (2)

Where,

$h_i$ is layer thickness

$\rho_i$ is layer resistiviy

3. **Coefficient of anisotropy**;

$\lambda = \left(\frac{\rho_t}{\rho_l}\right)^{1/2}$ (31, 32) (3)

Where,
$\rho_t$ is transverse resistance
$\rho_t$ is longitudinal conductance

The five parameters were integrated by calculating the average ratings of all the parameters after their summation at each VES locations. The final vulnerability average rating will then vary from 1 (low vulnerability) to 4 (high vulnerability).

## 4. RESULTS

Three to five geoelectric layers were delineated in the study area. The layers correspond to the topsoil, weathered layer (sandy clay and clayey sand), lateritic weathered layer, partially weathered basement/partially fractured basement and the presumed fresh bedrock. The layer's resistivity varies respectively from 38 to 845 ohm-m, 9 to 7490 ohm-m, 41 to 90224 ohm-m, 60 to 15191 ohm, 162 to 99668 ohm-m, while the layer thickness ranges from 0.4 to 5.2 m, 0.9 to 24.1 m, 2.8 to 30.4 m and 4.3 to 41.6 m (Table 1). Nine curve types were delineated across the study areas; A, H, K, HA, KH, AKH, HKA, HKH and KQH. H, A and KH are the predominant curve types in the area (Table 2 and Fig. 5).

**Table 2. Summary of Vertical Electric Sounding Results**

| VES No. | Res1 | Res2 | Res3 | Res4 | Res5 | h1 | h2 | h3 | Curve type |
|---|---|---|---|---|---|---|---|---|---|
| 1 | 249 | 93 | 982 | | | 1 | 4.1 | | H |
| 2 | 548 | 62 | 1527 | | | 1 | 3 | | H |
| 3 | 228 | 85 | 1636 | | | 1.3 | 8 | | H |
| 4 | 90 | 145 | 11238 | | | 1.1 | 6.7 | | A |
| 5 | 371 | 22 | 14991 | | | 1 | 2.3 | | H |
| 6 | 162 | 285 | 115 | 2227 | | 0.6 | 1.4 | 3.8 | KH |
| 7 | 169 | 86 | 2246 | | | 1.3 | 5.9 | | H |
| 8 | 309 | 82 | 1273 | | | 0.7 | 4.7 | | H |
| 9 | 193 | 363 | 77 | 989 | | 0.7 | 2.5 | 8.3 | KH |
| 10 | 191 | 104 | 813 | 1326 | | 0.5 | 1.5 | 14.9 | HA |
| 11 | 147 | 112 | 1145 | | | 0.8 | 7.3 | | H |
| 12 | 122 | 76 | 3863 | | | 1.3 | 3.3 | | H |
| 13 | 90 | 1413 | 1517 | | | 2.5 | 8.8 | | A |
| 14 | 148 | 34 | 2189 | | | 0.9 | 2.2 | | H |
| 15 | 850 | 95 | 2945 | | | 1.9 | 10.6 | | H |
| 16 | 141 | 203 | 52 | 1820 | | 0.8 | 2 | 10.1 | KH |
| 17 | 449 | 111 | 1199 | | | 1.4 | 12.2 | | H |
| 18 | 413 | 127 | 1587 | | | 2.7 | 12.2 | | H |
| 19 | 176 | 50 | 2914 | | | 1.5 | 16.7 | | H |
| 20 | 225 | 57 | 949 | | | 0.9 | 8.9 | | H |
| 21 | 135 | 41 | 1695 | 221 | 99656 | 0.7 | 1.2 | 9 | HKH |

| | | | | | | | | | |
|---|---|---|---|---|---|---|---|---|---|
| 22 | 156 | 78 | 315 | 60 | 711 | 0.9 | 1.2 | 2.5 | HKH |
| 23 | 236 | 81 | 5448 | | | 0.8 | 7.7 | | H |
| 24 | 137 | 76 | 2398 | | | 0.8 | 2.9 | | H |
| 25 | 221 | 1967 | 186 | 3376 | | 1.9 | 4.8 | 20.5 | H |
| 26 | 205 | 151 | 1170 | 312 | 5992 | 1.6 | 1.9 | 23.8 | HKH |
| 27 | 168 | 1203 | 176 | 1303 | | 1.9 | 8 | 25.4 | KH |
| 28 | 105 | 1809 | 95 | 714 | | 1.8 | 2.8 | 13 | KH |
| 29 | 214 | 445 | 185 | 1481 | | 2.3 | 6.3 | 14.3 | KH |
| 30 | 89 | 261 | 432 | 121 | 1771 | 2.2 | 1.8 | 3.5 | AKH |
| 31 | 105 | 936 | 457 | 16243 | | 1.2 | 3.3 | 4.6 | KH |
| 32 | 151 | 297 | 100 | 3208 | | 1.4 | 2.6 | 5.5 | KH |
| 33 | 134 | 866 | 89 | 3511 | | 1.6 | 2.7 | 8.8 | KH |
| 34 | 272 | 101 | 715 | 121 | 4687 | 0.5 | 0.9 | 2.8 | HKH |
| 35 | 121 | 44 | 1520 | | | 0.5 | 7.7 | | H |
| 36 | 122 | 84 | 2669 | | | 0.7 | 10.4 | | H |
| 37 | 68 | 25 | 303 | 1792 | 100000 | 1.4 | 2.4 | 30.9 | HKA |
| 38 | 421 | 225 | 359 | 83 | 1278 | 0.6 | 2.7 | 5.7 | HKH |
| 39 | 230 | 128 | 1723 | | | 1.9 | 20.4 | | H |
| 40 | 225 | 254 | 159 | 3539 | | 0.6 | 7 | 4.1 | KH |
| 41 | 412 | 60 | 679 | | | 1 | 3 | | H |
| 42 | 247 | 387 | 133 | 395 | | 0.6 | 2 | 8.1 | KH |
| 43 | 82 | 12.8 | 450 | 89806 | | 1.1 | 3 | 46.9 | HA |
| 44 | 308 | 206 | 670 | 174 | | 1.7 | 7.4 | 9.8 | HK |
| 45 | 89 | 173 | 1961 | | | 1.3 | 12 | | A |
| 46 | 212 | 124 | 3041 | | | 1.2 | 5.2 | | H |
| 47 | 567 | 6110 | 1686 | | | 0.6 | 5 | | K |
| 48 | 41 | 484 | 1086 | | | 1 | 7.2 | | A |
| 49 | 55 | 166 | 1633 | | | 1.8 | 20.6 | | A |
| 50 | 94 | 323 | 1336 | | | 1.1 | 25.7 | | A |
| 51 | 169 | 406 | 137 | 2175 | | 2 | 7 | 21.5 | KH |
| 52 | 148 | 553 | 2836 | | | 1.8 | 11.3 | | A |
| 53 | 120 | 174 | 2430 | | | 1.8 | 5.3 | | A |
| 54 | 130 | 60 | 4843 | | | 1.3 | 5.4 | | H |
| 55 | 98 | 21 | 30298 | | | 0.6 | 1.7 | | H |
| 56 | 142 | 93 | 90232 | | | 1.4 | 3.9 | | H |
| 57 | 395 | 216 | 656 | 3014 | | 0.5 | 2.7 | 20.3 | HA |
| 58 | 75 | 654 | 6039 | | | 1.6 | 4.7 | | A |
| 59 | 52 | 92 | 419 | | | 2.3 | 5.7 | | A |
| 60 | 47 | 330 | 42 | 2797 | | 1.5 | 4.3 | 11.5 | KH |

| | | | | | | | | | |
|---|---|---|---|---|---|---|---|---|---|
| 61 | 33 | 15 | 223 | | | 0.4 | 9.2 | | H |
| 62 | 100 | 276 | 69 | 5626 | | 2.7 | 7.4 | 25.5 | KH |
| 63 | 66 | 38 | 1656 | | | 1 | 6 | | H |
| 64 | 102 | 33 | 946 | | | 0.7 | 7.7 | | H |
| 65 | 105 | 27 | 592 | | | 1 | 7 | | H |
| 66 | 218 | 66 | 838 | | | 5.1 | 15 | | H |
| 67 | 90 | 42 | 1226 | | | 1 | 4.5 | | H |
| 68 | 229 | 103 | 361 | | | 3.5 | 15.7 | | H |
| 69 | 137 | 66 | 929 | | | 1.3 | 7.6 | | H |
| 70 | 227 | 66 | 780 | | | 5.2 | 12 | | H |
| 71 | 168 | 158 | 1328 | | | 1.3 | 6 | | H |
| 72 | 79 | 62 | 416 | | | 2.7 | 12.4 | | H |
| 73 | 211 | 101 | 378 | | | 2.5 | 12.4 | | H |
| 74 | 50 | 90 | 976 | | | 5.2 | 13.2 | | A |
| 75 | 120 | 3062 | 908 | 321 | 5130 | 1.3 | 3.3 | 3.9 | KQH |
| 76 | 95 | 187 | 3120 | | | 1 | 7.3 | | A |
| 77 | 89 | 102 | 1325 | | | 1.2 | 7.9 | | A |
| 78 | 221 | 428 | 7300 | | | 2.3 | 7.3 | | A |
| 79 | 85 | 1203 | 4999 | | | 1.2 | 16.4 | | A |
| 80 | 112 | 68 | 3811 | | | 5.3 | 5.6 | | H |
| 81 | 60 | 104 | 1012 | | | 1.4 | 4.8 | | A |
| 82 | 44 | 76 | 42 | 684 | | 1.1 | 1.9 | 15.6 | KH |
| 83 | 40 | 23 | 1451 | | | 0.8 | 7.6 | | H |
| 84 | 111 | 67 | 176 | | | 2.8 | 6.2 | | H |
| 85 | 209 | 142 | 327 | | | 4.6 | 11.9 | | H |
| 86 | 195 | 69 | 568 | | | 5 | 23 | | H |
| 87 | 67 | 56 | 2149 | | | 1.7 | 7.2 | | H |
| 88 | 347 | 69 | 2926 | | | 1.1 | 7.5 | | H |
| 89 | 120 | 99 | 1791 | | | 1.5 | 14.4 | | H |
| 90 | 154 | 141 | 613 | | | 1.6 | 37.7 | | H |
| 91 | 197 | 195 | 1149 | | | 3.7 | 14.7 | | H |
| 92 | 96 | 136 | 109 | 363 | | 1 | 4.1 | 17.9 | KH |
| 93 | 269 | 477 | 77 | 958 | | 1.9 | 3.7 | 16.9 | KH |
| 94 | 175 | 210 | 90 | 190 | | 1.9 | 4.6 | 9.3 | KH |
| 95 | 184 | 315 | 2023 | | | 2.8 | 17.6 | | A |

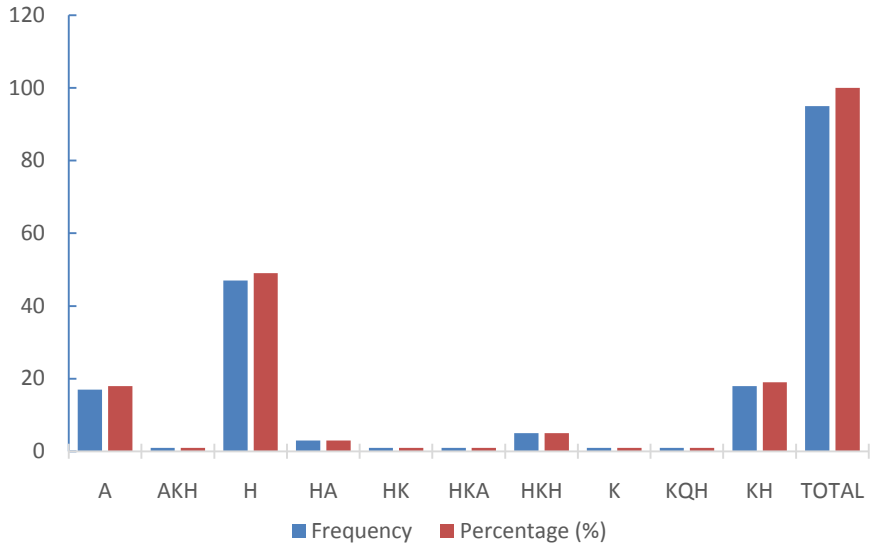


Fig. 5: The Frequency Range of the Curve Type obtained from the FUTA Campus

### 4.1 Vulnerability Assessment

Five parameters were integrated to predict the vulnerability of aquifer in the study area to possible contamination from the dump site. The first parameter is the aquifer overlying lithology which is inferred from layer resistivity values, the second parameter is point distance (of each VES location) from the dump site respectively. The remaining three parameters were second order geoelectric parameters; the transverse resistance, longitudinal conductance and coefficient of anisotropy. Table 3 shows the summary of these five parameters for each VES point. These parameters were presented as vulnerability maps. Each of the map divided the study area into four vulnerability zones (low, moderate, high and very high zones) based on the developed class interval as indicated in the thematic map.

**Table 3. Summary of Vulnerability model results**

| VES No | Transverse Resistance | Longitudinal Conductance | Coefficient of Anisotropy | Lithology | Distance From Dumpsite | Sum of Rating Values | Rating Average |
|---|---|---|---|---|---|---|---|
| 1 | 1 | 1 | 3 | 2 | 2 | 9 | 1.8 |
| 2 | 1 | 1 | 4 | 2 | 2 | 10 | 2 |
| 3 | 1 | 2 | 2 | 2 | 2 | 9 | 1.8 |
| 4 | 1 | 1 | 2 | 4 | 2 | 10 | 2 |
| 5 | 1 | 2 | 4 | 1 | 2 | 10 | 2 |
| 6 | 1 | 1 | 1 | 1 | 2 | 6 | 1.2 |
| 7 | 1 | 1 | 2 | 1 | 2 | 7 | 1.4 |
| 8 | 1 | 1 | 3 | 1 | 2 | 8 | 1.6 |
| 9 | 1 | 2 | 4 | 2 | 2 | 11 | 2.2 |
| 10 | 3 | 1 | 4 | 1 | 3 | 12 | 2.4 |
| 11 | 1 | 1 | 1 | 2 | 3 | 8 | 1.6 |

| | | | | | | | |
|---|---|---|---|---|---|---|---|
| 12 | 1 | 1 | 2 | 1 | 3 | 8 | 1.6 |
| 13 | 3 | 1 | 4 | 1 | 3 | 12 | 2.4 |
| 14 | 1 | 1 | 4 | 1 | 3 | 10 | 2 |
| 15 | 2 | 2 | 4 | 1 | 3 | 12 | 2.4 |
| 16 | 1 | 3 | 4 | 1 | 3 | 12 | 2.4 |
| 17 | 1 | 2 | 3 | 1 | 3 | 10 | 2 |
| 18 | 2 | 2 | 3 | 1 | 3 | 11 | 2.2 |
| 19 | 1 | 4 | 2 | 2 | 3 | 12 | 2.4 |
| 20 | 1 | 3 | 3 | 2 | 3 | 12 | 2.4 |
| 21 | 1 | 2 | 1 | 1 | 2 | 7 | 1.4 |
| 22 | 1 | 2 | 1 | 1 | 1 | 6 | 1.2 |
| 23 | 1 | 2 | 2 | 2 | 2 | 9 | 1.8 |
| 24 | 1 | 1 | 2 | 2 | 2 | 8 | 1.6 |
| 25 | 3 | 2 | 4 | 4 | 2 | 15 | 3 |
| 26 | 1 | 3 | 1 | 4 | 2 | 11 | 2.2 |
| 27 | 3 | 3 | 3 | 4 | 2 | 15 | 3 |
| 28 | 2 | 3 | 4 | 4 | 3 | 16 | 3.2 |
| 29 | 2 | 2 | 1 | 4 | 3 | 12 | 2.4 |
| 30 | 2 | 2 | 4 | 4 | 3 | 15 | 3 |
| 31 | 2 | 1 | 4 | 1 | 3 | 11 | 2.2 |
| 32 | 1 | 1 | 3 | 2 | 2 | 9 | 1.8 |
| 33 | 2 | 2 | 4 | 1 | 4 | 13 | 2.6 |
| 34 | 2 | 1 | 4 | 1 | 4 | 12 | 2.4 |
| 35 | 1 | 3 | 2 | 3 | 4 | 13 | 2.6 |
| 36 | 1 | 2 | 1 | 2 | 2 | 8 | 1.6 |
| 37 | 4 | 3 | 4 | 1 | 4 | 16 | 3.2 |
| 38 | 2 | 3 | 4 | 2 | 1 | 12 | 2.4 |
| 39 | 2 | 3 | 2 | 1 | 1 | 9 | 1.8 |
| 40 | 2 | 1 | 2 | 1 | 2 | 8 | 1.6 |
| 41 | 1 | 1 | 4 | 1 | 2 | 9 | 1.8 |
| 42 | 1 | 1 | 3 | 1 | 1 | 7 | 1.4 |
| 43 | 4 | 4 | 4 | 1 | 2 | 15 | 3 |
| 44 | 3 | 1 | 4 | 4 | 2 | 14 | 2.8 |
| 45 | 1 | 1 | 2 | 1 | 3 | 8 | 1.6 |
| 46 | 1 | 1 | 2 | 1 | 3 | 8 | 1.6 |
| 47 | 4 | 1 | 4 | 1 | 3 | 13 | 2.6 |
| 48 | 2 | 1 | 4 | 4 | 2 | 13 | 2.6 |
| 49 | 2 | 3 | 2 | 2 | 3 | 12 | 2.4 |
| 50 | 2 | 1 | 2 | 4 | 3 | 12 | 2.4 |
| 51 | 2 | 3 | 3 | 2 | 3 | 13 | 2.6 |
| 52 | 2 | 1 | 3 | 1 | 3 | 10 | 2 |
| 53 | 1 | 1 | 2 | 4 | 3 | 11 | 2.2 |

| | | | | | | | |
|---|---|---|---|---|---|---|---|
| 54 | 1 | 2 | 2 | 1 | 3 | 9 | 1.8 |
| 55 | 1 | 1 | 4 | 1 | 3 | 10 | 2 |
| 56 | 1 | 1 | 2 | 1 | 4 | 9 | 1.8 |
| 57 | 3 | 1 | 2 | 1 | 3 | 10 | 2 |
| 58 | 2 | 1 | 4 | 1 | 4 | 12 | 2.4 |
| 59 | 1 | 2 | 2 | 1 | 4 | 10 | 2 |
| 60 | 1 | 4 | 4 | 1 | 4 | 14 | 2.8 |
| 61 | 1 | 4 | 2 | 1 | 4 | 12 | 2.4 |
| 62 | 2 | 4 | 4 | 3 | 4 | 17 | 3.4 |
| 63 | 1 | 3 | 2 | 1 | 1 | 8 | 1.6 |
| 64 | 1 | 4 | 2 | 1 | 1 | 9 | 1.8 |
| 65 | 1 | 4 | 3 | 3 | 1 | 12 | 2.4 |
| 66 | 1 | 4 | 4 | 1 | 1 | 11 | 2.2 |
| 67 | 1 | 2 | 2 | 1 | 1 | 7 | 1.4 |
| 68 | 1 | 3 | 2 | 3 | 1 | 10 | 2 |
| 69 | 1 | 2 | 2 | 3 | 1 | 9 | 1.8 |
| 70 | 1 | 3 | 4 | 1 | 1 | 10 | 2 |
| 71 | 1 | 1 | 1 | 1 | 1 | 5 | 1 |
| 72 | 1 | 3 | 1 | 3 | 1 | 9 | 1.8 |
| 73 | 1 | 2 | 2 | 3 | 1 | 9 | 1.8 |
| 74 | 1 | 4 | 2 | 3 | 1 | 11 | 2.2 |
| 75 | 3 | 1 | 4 | 2 | 4 | 14 | 2.8 |
| 76 | 1 | 1 | 2 | 1 | 4 | 9 | 1.8 |
| 77 | 1 | 1 | 1 | 4 | 3 | 10 | 2 |
| 78 | 2 | 1 | 2 | 2 | 3 | 10 | 2 |
| 79 | 3 | 1 | 4 | 1 | 3 | 12 | 2.4 |
| 80 | 1 | 2 | 2 | 1 | 3 | 9 | 1.8 |
| 81 | 1 | 1 | 2 | 1 | 3 | 8 | 1.6 |
| 82 | 1 | 4 | 2 | 2 | 4 | 13 | 2.6 |
| 83 | 1 | 4 | 2 | 2 | 2 | 11 | 2.2 |
| 84 | 1 | 2 | 2 | 4 | 2 | 11 | 2.2 |
| 85 | 2 | 2 | 2 | 2 | 2 | 10 | 2 |
| 86 | 2 | 4 | 3 | 2 | 2 | 13 | 2.6 |
| 87 | 1 | 3 | 1 | 1 | 2 | 8 | 1.6 |
| 88 | 1 | 2 | 4 | 1 | 2 | 10 | 2 |
| 89 | 1 | 3 | 1 | 1 | 2 | 8 | 1.6 |
| 90 | 2 | 4 | 1 | 1 | 1 | 9 | 1.8 |
| 91 | 2 | 1 | 1 | 1 | 2 | 7 | 1.4 |
| 92 | 2 | 3 | 1 | 1 | 1 | 8 | 1.6 |
| 93 | 2 | 3 | 4 | 1 | 1 | 11 | 2.2 |
| 94 | 1 | 2 | 3 | 1 | 1 | 8 | 1.6 |
| 95 | 2 | 1 | 2 | 1 | 1 | 7 | 1.4 |

### 4.2 Aquifer Overlying Lithology

The lithology or physical characteristics of the rock formations underlying an area can have a significant impact on its vulnerability (16, 18). The physical and chemical properties (porosity, permeability and sorption) of the subsurface layer can affect the movement of groundwater and contaminants through them (15, 16). Four lithological units; quartzite, charnockite, migmatite-gneiss and granite were recognized in the study area (See Fig. 3). The topsoil and weathered materials in the basement environment are always a reflection of the underlying geology, since they are formed in-situ. Quartzite derived soil will be sandy and consequently have higher porosity and permeability. While migmatite-gneiss derived soil and granite derived soil will have lower permeability because these weathered materials will contain more of clay and less of sand. Charnockite derived soil is expected to be porous and less permeable because it will contain more clay than sand. The porosity and permeability of weathered material can affect their ability to absorb and transport fluids. When porosity and permeability of the aquifer overlying layers are high, then the underlying aquifer will be more vulnerable to leachate contamination, conversely, when permeability is low in overlying layer, then the aquifer layer will be less vulnerable to leachate contamination (16, 18).

### 4.3 Point Distance from Dumpsite

Various types of waste materials are dump indiscriminately at dumpsites, including household garbage, industrial waste and hazardous chemicals. Over time, these waste materials get decay and produced leachate. These leachates can percolate into the subsurface and reach the groundwater causing contamination. The leachate can also flow laterally through the surface and subsurface. The closer a location is to the dumpsite the higher the possibility that the point will be contaminated by leachate emanating from the dump site. In the study area, the distance from dumpsite ranges from 433.7 to 3613.9 m (Fig. 6). A total of 21 VES locations fall under area with low vulnerability, 30 VES points fall under area with medium vulnerability, and 31 VES points fall under area with high vulnerability and the remaining 13 VES points falls under area with very high vulnerability.

### 4.4 Transverse Resistance

Transverse resistance refers to the ability of subsurface materials (such as soil or rock) to resist the vertical movement of contaminants through the topsoil and subsurface, and get to the aquifer layer. This resistance is typically determined by the permeability of the subsurface materials and more importantly the mineralogical content of the geologic materials making up the subsurface layers. Higher transverse resistance indicates that the subsurface materials are sandier and less clayey. Therefore, such subsurface materials will allow easy passage of contaminant plume through them into the underlying aquifer layer. Thus, the higher the transverse resistance the higher the overall vulnerability of the area to contamination (33, 34).The total transverse resistance (T) map (Fig. 7) of the study area was generated using the interpolation technique in ArcGIS environment. The Fig. shows the spatial variation of the transverse resistance within the study area ranges between 85 - 48830 Ωm. The produced map shows that the blue zones around the Northwest and south western side of the map with 85 - 2470 Ωm are predominantly low transverse resistance, the light green shows medium transverse resistance with 2471 - 8423 Ωm, while the yellow shows high transverse resistance with values (8424 - 21071 Ωm) and the red around the south eastern part of the map showing very high transverse resistance greater than 21072 Ωm.

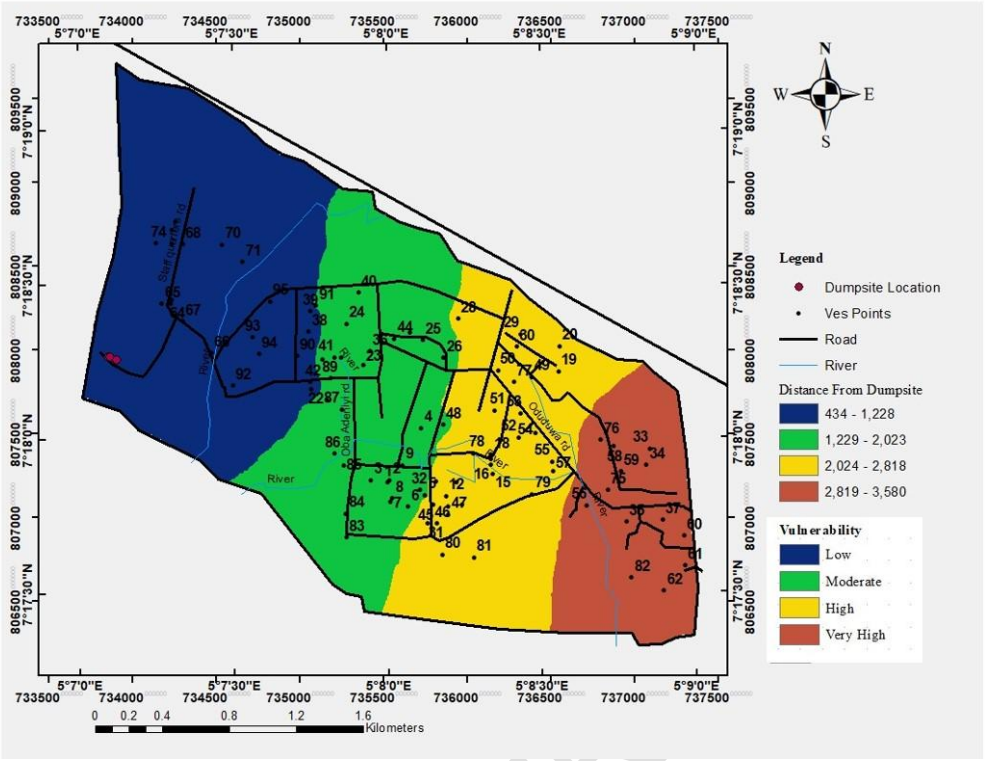


Fig. 6. Distance of VES points from dumpsite

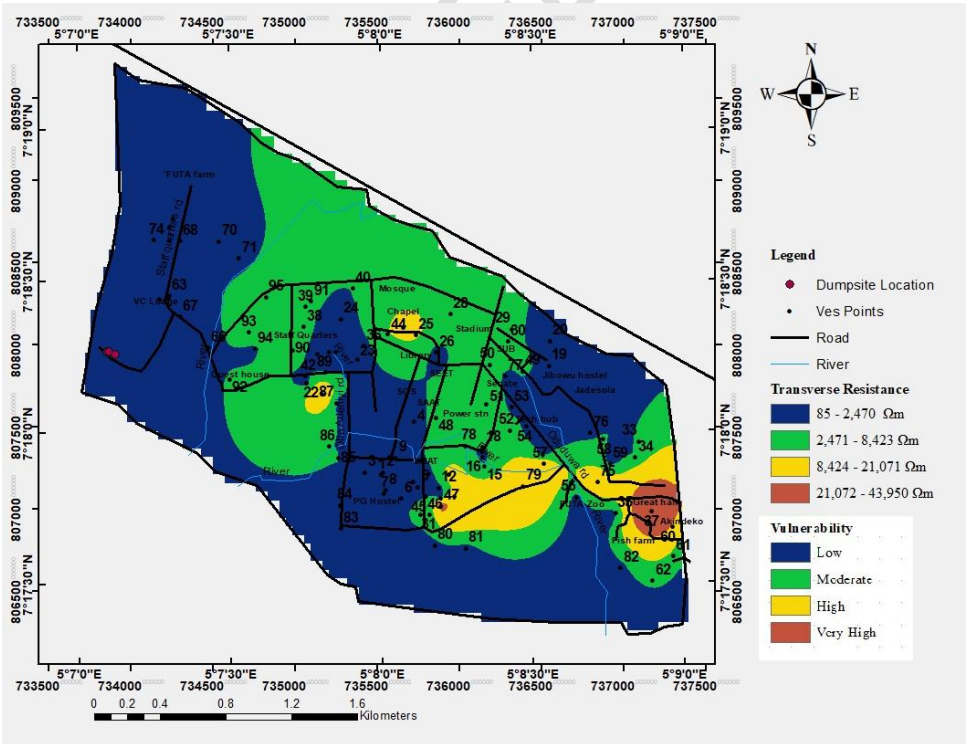


Fig. 7: Transverse Resistance Map of FUTA Campus

## 4.5 Longitudinal Conductance

Longitudinal conductance values range from 0.0102 - 0.559 mhos (Fig. 8). Higher longitudinal conductance indicates that the subsurface geologic materials are conductive and allow free passage of electric current. These suggests that geologic material associated with high longitudinal conductance consist more of clay minerals which are capable of holding on to contaminants plume. Therefore, zones with high longitudinal conductance values are less vulnerable to contamination (33, 34). Generally, the area is zone into four based on class distribution of LC, the blue-coloured zones indicate zones of very high (0.239 - 0.559 mhos) LC values around the central to southern parts of the map with the green showing area of high (0.149 - 0.238 mhos) LC values, the yellow colour showing areas around the edges of the map to the north west and south east with moderate (0.0966 - 0.148 mhos) LC around the south eastern end of the map with red colour showing low (0.0102 - 0.0965 mhos) values of LC.

## 4.6 Coefficient of Anisotropy

The coefficient of anisotropy refers to a measure of the degree of anisotropy or directional variability in the hydraulic conductivity of subsurface materials. Hydraulic conductivity is a measure of the ability of a subsurface material (such as soil or rock) to transmit water and it can vary in different directions depending on the orientation of the subsurface materials. The coefficient of anisotropy is defined as the ratio of the hydraulic conductivity in the direction of maximum permeability to the hydraulic conductivity in the direction of minimum permeability. Fig. 8 shows the anisotropic coefficient map of the study area. The coefficient of anisotropy is an important factor in assessing vulnerability because it can influence the flow of contaminants through the subsurface. For example, if the subsurface materials have a high coefficient of anisotropy, contaminants will travel more quickly in the direction of higher permeability, potentially increasing the vulnerability of the area to contamination (33, 34). Therefore, an understanding of the coefficient of anisotropy can be important for assessing and managing potential contamination risks. In the coefficient of anisotropy (COA) map (Fig. 10), the study area was characterized into four zones. The COA values in the area range from 0.2778 to 1.858. The southern flank is characterized by low COA (0.2778 - 1.009) values, which can be attributed principally to the influence of the shallow bedrock and adjacent fluid-saturated reservoirs (Fig. 9). However, the northwestern flank exhibits a very high COA (1.14 - 1.858), which extends eastward through the center, with pocket in of low values at the southern parts. The area with high values of COA suggests that the fracture system must have extended in all the directions with different degrees of fracturing, which had greater water-holding capacity from different directions of the fracture(s) within the rock resulting in higher porosity and thus higher vulnerability.

## 4.7 Vulnerability Model Map

The vulnerability model map was generated using the modified Le Grand vulnerability model (LGVM) earlier discussed. The vulnerability model map integrated all the parameters together (See Table 3) into one single map (Fig. 10) using simple approach of Le Grand model. The western part of the map showed low overall vulnerability with spots of moderate venerability. A sizeable strip running from the north-south across the central of the study area showed overall moderate vulnerability. Areas with high and very high vulnerability are spread out and interwoven across the north east to south eastern part of the study area

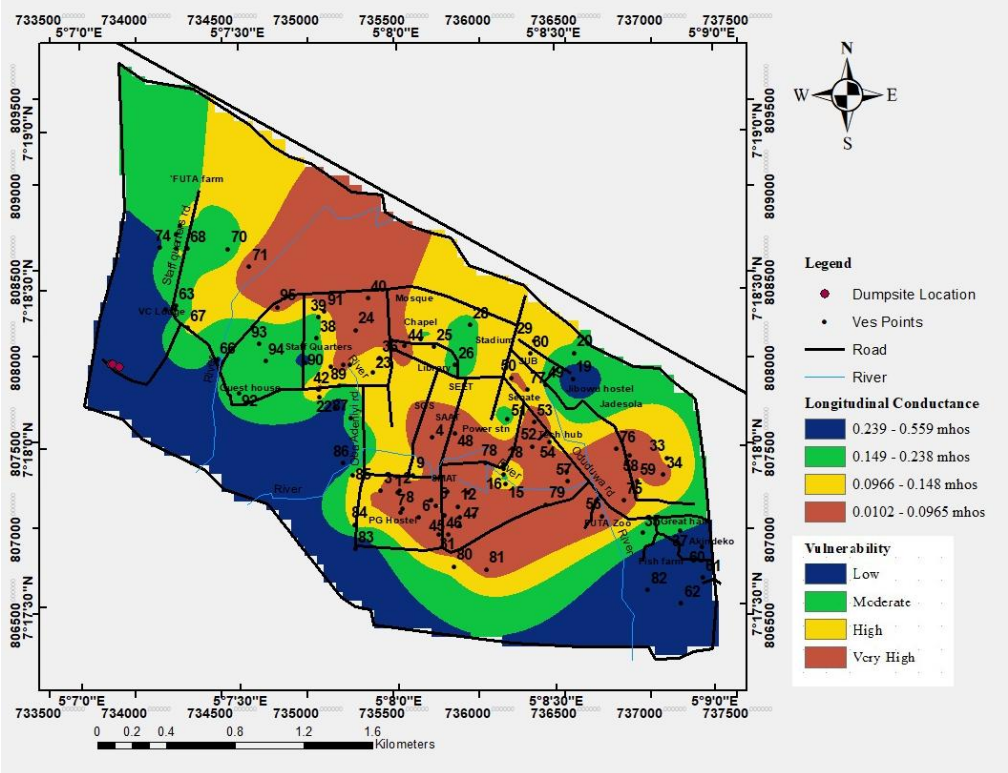


Fig. 8: Longitudinal Conductance Map of FUTA Campus

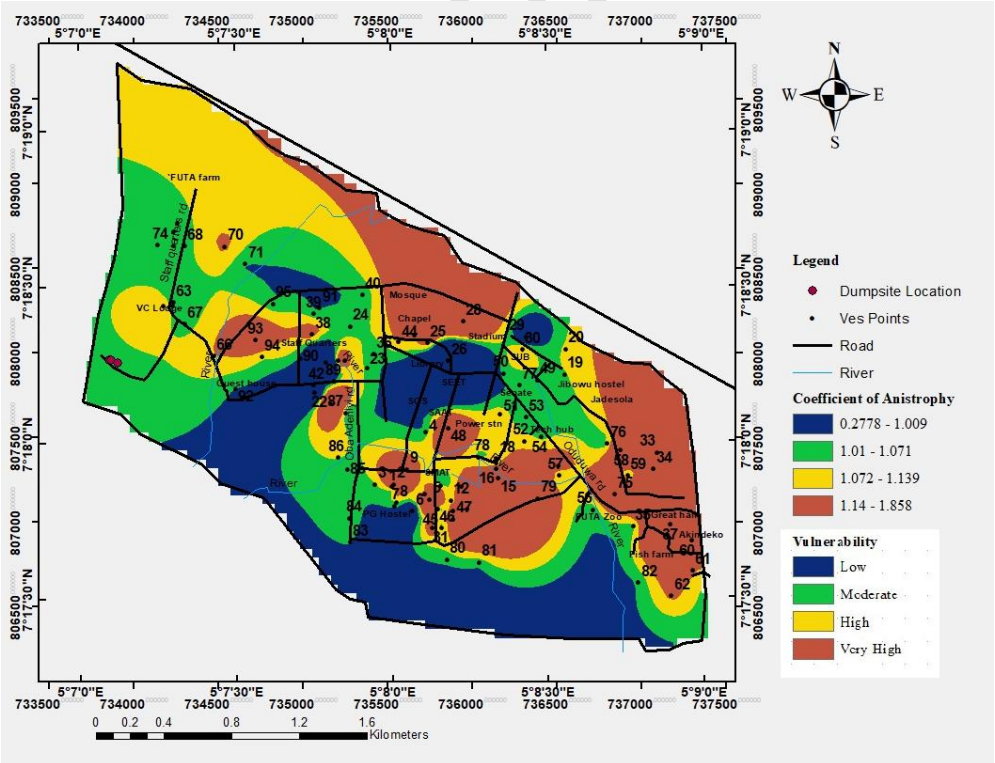


Fig. 9: Coefficient of Anisotropy Map of FUTA Campus

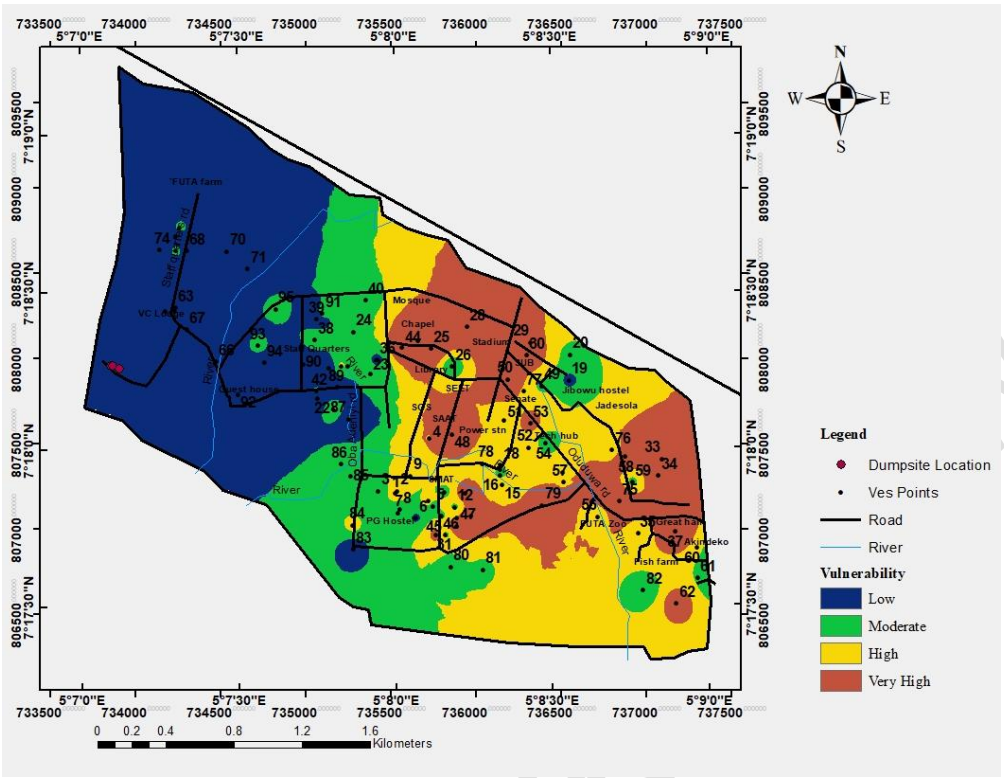


Fig. 10: Aquifer Venerability Model Map of FUTA Campus

### 4.8 Vulnerability Model Map Validation

The vulnerability model map validation was done using the hydro-chemical analysis of water samples obtained from 8 wells across the study area. Two (2) water samples were collected from each vulnerability zones based on the vulnerability model map (Fig. 10). Three (3) physio-chemical parameters considered for validation exercise are total dissolved solid (TDS), electrical conductivity (EC) and total hardness (TH). The results of the physio-chemical analysis of the groundwater samples are as presented in table 4 and their concentration were compared with the WHO standard (35, 36; Table 5).

**Table 4. Hydro-chemical analysis of water sample across vulnerability zone in the study area**

| S/N | Sample ID | TDS | EC | TH | Temperature | Vulnerability |
|---|---|---|---|---|---|---|
| 1 | PG Hostel | 68 | 136 | 50 | 30.3 | Low |
| 2 | Guest House | 104 | 208 | 52.5 | 30.1 | Low |
| 3 | FUTA Farm | 239 | 368 | 148 | 30.4 | Moderate |
| 4 | Staff Quarters | 95 | 146 | 54 | 30.1 | Moderate |
| 5 | Akindeko Hall | 147 | 226 | 116 | 30 | High |
| 6 | SAAT | 91 | 140 | 60 | 29.5 | High |
| 7 | Fish Farm | 102 | 204 | 54 | 30 | Very High |
| 8 | Sport Complex | 65 | 130 | 47.5 | 30.3 | Very High |

**Table 5. Vulnerability model map validation**

| S/N | Sample Location | Vulnerability Zone | Model Agreement with Water Analysis |
|---|---|---|---|
| 1 | PG Hostel | Low | Agree |
| 2 | Guest House | Low | Agree |
| 3 | FUTA Farm | Moderate | Agree |
| 4 | Staff Quarters | Moderate | Agree |
| 5 | Akindeko Hall | High | Agree |
| 6 | SAAT | High | Agree |
| 7 | Fish Farm | Very High | Agree |
| 8 | Sport Complex | Very High | Agree |



## 5. CONCLUSION AND RECOMMENDATIONS

The work is aim at assessing possible impact of FUTA dumpsite on groundwater resources within the campus. Vertical electrical sounding was done across the study area in 94 locations. The VES results enabled the delineation of different geoelectric layers beneath the study area, identification of aquifer layer(s) where present, identification of the overlaying lithology above the aquifer layer across the area, determination of the transverse resistance, aquifer total overburden longitudinal conductance, coefficient of anisotropy, lithology and VES distances from the dumpsite.

Overlying lithology, transverse resistance, total overburden longitudinal conductance, coefficient of anisotropy and VES distances from the dumpsite. These five (5) parameters were combined using the Le Grand model chart to evaluate and generate aquifer venerability model across the study area. The study area was divided into four zones of vulnerability based on our successful classification efforts: low, moderate, high and very high. The dumpsite is located in an area with low vulnerability and also in a relatively low elevated area (See Fig. 2) which eliminate possibility leachate outward migration or outflow of leachate from the dumpsite. The aquifer venerability model map was validated using physio-chemical analysis results. The water samples analyzed were all within WHO desirable and permissible limits (35, 36) for potable water.

## REFERENCES


1. Abdullahi, NK, Osazuwa, IB, Sule, PO, &Onugba, A. 2013. Geophysical Assessment of an Active Open Dumpsite in Basement Complex of Northwestern Nigeria. *International Journal of Engineering Science Invention. 2013;*2(5):12-2.
2. Adebowale, EA, Folorunso, AF, Kayode, OT. Integrated Geophysical and Geochemical methods for Environmental Assessment of Municipal Dumpsite System. *International Journal of Geosciences*. 2013;4:850-862.
3. Adebayo, AS, Ariyibi, EA, Awoyemi, MO, Onyedim, GC. Delineation of Contaminant Plumes at Olobonku Dumpsite Using Geophysical and Geochemical Approach at Ede Town, Southwestern Nigeria. *Geosciences*. 2015;5(1):39-40.
4. Adeniran, AO, Oyenade, H. (2016). Inventory analysis of solid waste management in Ikorodu community. *Civil and Environmental Research*. 2016;8(9):26-38.
5. Olayanju, GM, Olla, TA, Akinlalu, AA, Adelusi, AO, Adiat, KA. Geophysical and Hydrochemical Investigation of a Municipal Dumpsite in Ibadan, Southwestern Nigeria. *Journal of Environment and Earth Science*.2015;5(14):99-112.
6. Shemang, EM, Molwalefhe, L, Chaoka, TR, Mosweu, E,Nondo, M. Geophysical Investigation of the Old Gaborone Dumpsite, Botswana. *Journal of Applied Science, and Environmental*.2006;10(3):87-92.
7. Zekster, IS, Everest, LG. (2004). Groundwater Resources of the World and Their Use, 1HP - VI, Series on Groundwater No. 6. UNESCO (United Nations Educational, Scientific and Cultural Organization). 2004;342.
8. Eyankware, MO, Ogwah, C, Selemo, AOI.Geoelectrical Parameters for the Estimation of Groundwater Potential in Fracture Aquifer at Sub-Urban Area of Abakaliki, SE Nigeria. *Int. Journ. Earth Sci. Geophys*. 2020;(6):31.
9. Olayanju, GM, Ojo, AO. Magnetic Characterization of Rocks Underlying FUTA Campus Southwest Nigeria. Journal of Environment and Earth Science (JEES), of *International Institute for Science, Technology and Education* (IISTE), *Journal of Environment and Earth Science*. 2015;5(14):113-127.
10. Le Grand, E. H. (1964). System for Evaluation of Contamination Potential of Some Waste Disposal Sites. A paper presented on Nov. 8, 1963, at the Chesapeake Section Meeting, Washington, Water Resources Div., USGS, Washington, D.C
11. Salufu, SO, Okoduwa, SO, Okanigbuan, PN, Oko, C. (2022). Application of Legrand pollution correlation in the evaluation of contaminants migration within the groundwater of Ebhoakhuala in Ekpoma and Agbede, Edo State, Nigeria. 2022:7.
12. Van Stempvoort, DL, & Evert, LW. Aquifer vulnerability index: A GIS compatible method for groundwater vulnerability mapping. *Canada Water Resource Journal*. 1993;18:25-37.
13. Foster, SSD. Fundamental concepts in aquifer vulnerability, pollution risk and protection strategy. *Hydrol. Resour. Proc. Inf*. 1987;38:69-86.
14. Huan, H, Wang, J,Teng, Y. Assessment and validation of groundwater vulnerability to nitrate based on a modified DRASTIC model: a case study in Jilin City of northeast China. *Science of the Total Environment.* 2012;440:14-23.
15. Omosuyi, G.O, Oseghale, A. Groundwater Vulnerability Assessment in Shallow Aquifers using Geoelectric and Hydrogeologic Parameters at Odigbo, Southwestern Nigeria, *In Am. J. Sci. Ind. Res*. 2012;3(6):501-512.
16. Adeyemo, IA, Olowolafe, TS, Fola-Abe, AO. Aquifer Vulnerability Assessment at Ipinsa-Okeodu Area, Near Akure, Southwestern Nigeria, Using GODT, *International Journal of Environmental and Earth Science*. 2016;6(6): 9-18.
17. Mogaji, KA, Omobude, OB. Modeling of Geoelectric Parameters for Assessing Groundwater Potentiality in a Multifaceted Geologic Terrain, Ipinsa Southwest, Nigeria - A GIS-based GODT approach," In NRIAG *Journal of Astronomy and Geophysics*. 2017;6:2, 434-451, DOI: 10.1016/j.nrjag.2017.07.001, 2017.

18. Oni, TE,Omosuyi, GO, Akinlalu, AA. Groundwater Vulnerability Assessment Using Hydrogeologic and Geoelectric Layer Susceptibility Indexing at IgbaraOke, Southwestern Nigeria. *NRIAG Journal of Astronomy and Geophysics*. 2017;6(2), 452-458. https://doi.org/10.1016/j.nrjag.2017.04.009
19. Civita, M. LegendaUnificata per le Carte Della Vulnerabilita' deiCorpiIdriciSotterranei/Unified Legend for the Aquifer Pollution Vulnerability Maps. StudisullaVulnerabilita' degliAcquiferi, 1 (Append.); Pitagora: Bologna, Italy. 1990;13.
20. Napolitano, P. GIS for aquifer vulnerability assessment in the PianaCampana, southern Italy, using the DRASTIC and SINTACS methods. MSc Thesis, Enschede, The Netherlands, *International Institute for Geo-Information Science and Earth Observation(ITC)*, 1995;172p
21. Civita, M, De Regibus, C. Sperimentazione di alcunemetodologie per la valutazionedellavulnerabilitàdegliaquiferi. Q Geol. Appl. Pitagora Bologna. 1995;(3):1995;63-71.
22. Civita, M, De Maio, M. SINTACS. Un SistemaParametrico per la Valutazione e la Cartografia Della Vulnerabilita' DegliAcquiferiAll'inquinamento. Metodologia and Automatizzazione; Pitagora, Bologna, Italy.1997.
23. Civita, M, De Maio, M. SINTACS R5-Valutazione e CartografiaAutomatica Della VulnerabilitàDegliAcquiferiAll'inquinamento con ilSistemaParametrico; Pitagora: Bologna, Italy, 2000;226-232.
24. Civita, M. The combined approach when assessing and mapping groundwater vulnerability to contamination. *Journ. Water Resour.* Prot. 2, 2010;(2):14-28.
25. Corniello, A,Ducci, D,Monti, GM. Aquifer pollution vulnerability in the Sorrento Peninsula, Southern Italy, evaluated by SINTACS Method. Geof*í*s. Int. 2004;(43):575-581.
26. Al Kuisi, M, El-Naqa, A; Hammouri, N. Vulnerability mapping of shallow groundwater aquifer using SINTACS model in the Jordan Valley area, Jordan. Environ. Geol. 2006;(50):651-667.
27. Rosen, L. A study of the DRASTIC methodology with emphasis on Swedish conditions. *Groundwater*.1994;32(2):278-285.
28. Secunda, S., Collin, M, Melloul, A. Groundwater vulnerability assessment using a composite model combining DRASTIC with extensive agricultural land use in Israel's Sharon region. *Journ. Environ Manag.*1998;54(1):39-57
29. Thirumalaivasan, D, Karmegam, M, Venugopal, K. AHP-DRASTIC: Software for Specific Aquifer Vulnerability Assessment Using DRASTIC Model and GIS. Environmental Model & Software, 2003;18 (7):645-656.
30. Saha, D, Alam, F. Groundwater vulnerability assessment using DRASTIC and Pesticide DRASTIC models in intense agriculture area of the Gangetic plains India. *Environ. Monit. Assess.*2014;186(12),8741-8763.
*31.* Zohdy, AAR, Eaton, GP, Mabey, DR. Application of Surface Geophysics to Ground-Water Investigations, In Techniques of Water-Resources Investigations of the United States Geological Survey. 1974; Book 2, Chapter D1. 63p.
32. Kalinski, R, Kelly, W, Bogardi, I, Ehrman, R, Yamamoto, D. Correlation between DRASTIC vulnerabilities and incidents of VOC contamination of municipal wells in Nebraska. *Groundwater*. 1994;32(1):31-34.
33. Henriet, JP. Direct Application of Dar Zarrouk Parameters in Groundwater Survey. *Geophys. Prospect.*1976*;(*24):344-353.
34. Oladapo, MI, Mohammed, MZ, Adeoye, OO, Adetola, OO. Geoelectric Investigation of the Ondo State Housing Corporation Estate; Ijapo, Akure, Southwestern *Nigeria. J. Mining Geol*ogy. 2004;(40)41-48.
35. World Health Organization. International Standards for Drinking Water Quality. 1, Geneva. 1984:130p.

36. World Health Organization. Water and Sanitation. Guidelines for Drinking Water Quality, 3rd Edition. Geneva, Switzerland. 2008:668p.
37. Sandeep K, Athira AS, Arshak AA, Reshma KV, Aravind GH, Reethu M. Geoelectrical and hydrochemical characteristics of a shallow lateritic aquifer in southwestern India. Geosystems and Geoenvironment. 2023 May 1;2(2):100147.
38. Akiang FB, Emujakporue GO, Nwosu LI. Leachate delineation and aquifer vulnerability assessment using geo-electric imaging in a major dumpsite around Calabar Flank, Southern Nigeria. Environmental Monitoring and Assessment. 2023 Jan;195(1):123.